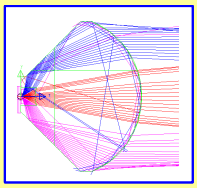

Ventura Photonics

Photonics Solutions

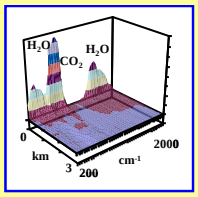

A Null Hypothesis for CO_2

Roy Clark PhD

Ventura Photonics Climate Note 2, VPCN 002.1
Ventura Photonics
Thousand Oaks, CA
September 2019

The prevailing hypothesis in climate science is based on the concept of radiative convective equilibrium. Some kind of average equilibrium climate state is assumed to exist in which the surface temperature is determined by an exact flux balance between the absorbed solar flux and the emission of long wave IR (LWIR) radiation back to space. When this climate state is perturbed by the addition of more greenhouse gases such as CO_2 to the atmosphere, the system adjusts to a new state with a higher surface temperature. This response is amplified by water vapor feedback [IPCC, 2013]. Simple comparison of climate model results with the surface temperature record show that this hypothesis has failed [Christie, 2019; Spencer, 2013].

A null hypothesis for CO_2 is therefore introduced, based on a description of the earth's climate in terms of dynamically coupled thermal reservoirs [Clark, 2019a, b, c, 2013 a, b]. The underlying principle is that a change in temperature is produced by a change in the heat content or enthalpy of a thermal reservoir divided by the heat capacity. The change in heat content is produced by the change in the total heat flux coupled to the reservoir over a given time period. The various flux terms cannot be separated and analyzed independently. Small increases in the LWIR flux from an increase in atmospheric CO_2 concentration have to be included in the total, time dependent flux terms. They are then too small to cause a measurable change in surface temperature.

The earth's climate is determined by a subtle dynamic or time dependent balance between the solar heating and the wind driven evaporative cooling of the oceans as the ocean water is circulated through the ocean gyres. There can never be an exact flux balance and the surface temperatures within the gyres must undergo quasi-periodic oscillations. The observed temperature recovery from the Maunder minimum has been caused by a small increase in solar flux. This is the result of changes in the sunspot index and other measures of solar activity.

Over longer time scales, the solar flux balance also changes with the ellipticity of the earth's orbit and the axial tilt and precession of the earth's rotation axis (Milankovitch cycles). In the recent

geological past, this has cycled the earth through a series of Ice Ages with a period of approximately 100,000 years. In addition, the plate tectonic motion of the continents since the breakup of the supercontinent of Pangaea starting about 170 million years ago has produced climate change through the alteration of the ocean gyre circulation [Zachos et al, 2001]. In much earlier geological times, about 2.5 billion years ago the solar flux was only 80% of its current value. However, the earth at the time remained relatively warm with little glaciation. This may be explained in terms of ocean wind driven evaporative cooling. There can be no 'young sun paradox' because the surface temperature is not controlled by the LWIR flux [Goldblatt and Zahnle, 2011].

The null hypothesis has 2 parts:

1) It simply impossible for the observed 120 ppm increase in atmospheric CO_2 concentration to have produced any measurable increase in surface temperature.

2) The observed recovery in surface temperature since the Maunder minimum can be explained in terms of small increases in the solar flux absorbed and accumulated in the ocean thermal reservoir.

The two parts of this null hypothesis will now be considered in turn.

Part 1: It simply impossible for the observed 120 ppm increase in atmospheric CO_2 concentration to have produced any measurable increase in surface temperature.

This can be demonstrated quite simply by calculating the surface temperature from first principles using the time dependent surface flux balance. The surface reservoir is heated by the absorbed solar flux and cooled by a combination of net LWIR emission, convection or sensible heat flux and evaporation or latent heat flux.

The air-land and the air-ocean interfaces have rather different thermal properties and have to be treated separately. Over land, the solar heating is limited to a thin surface layer. This establishes thermal gradient at the surface with the cooler air above that drives the convection. In addition. Heat is conducted below the surface. Later in the day the subsurface thermal gradient reverses and the stored heat is returned to the surface. Over the oceans, the water surface is almost transparent to the solar flux. Approximately half of the solar flux is absorbed in the first meter layer of the ocean and 90% is absorbed within the first 10 m layer. However, the LWIR flux and the wind driven evaporation are mixed together within the first 100 μm surface layer [Hale and Querry, 1973]. The cooler water produced at the surface by the combined cooling fluxes then sinks and cools the bulk ocean layers below. This is a Rayleigh-Benard convection process, not simple diffusion.

Over the last 200 years, the atmospheric concentration of CO_2 has increased by about 120 ppm from 280 to 400 ppm [Keeling, 2019]. This has produced an increase of approximately 2 W m^{-2}

in the downward LWIR flux from CO_2 reaching the surface [Clark, 2013a; 2013b; 2011; Harde. 2017]. Over the oceans, this small increase in flux is mixed with the wind driven evaporation and cannot penetrate below the surface. The increase in wind speed needed to compensate for the ocean surface warming produced by a 2 W m^{-2} increase in LWIR flux is shown in Figure 1. This is based on a thermal engineering analysis of the ocean surface temperature discussed in detail by Clark [2019a, b]. The blue curve shows the increase in wind speed needed when a fixed LWIR window cooling flux of 45 W m^{-2} is used at all latitudes and reduced to 43 W m^{-2} to simulate the change in CO2 LWIR flux. The orange curve shows the increase in wind speed using a temperature dependent LWIR window flux that increases by 2.2 W m^{-2} for each 1 C rise in surface temperature. The important point to note is that up to 30° latitude, the change in wind speed is below 10 CENTIMETERS per second. Typical variation in wind speed is 1 to 12 meters per second, with higher wind gusts. This is at least a factor of 10 to 100 larger than that needed to dissipate the 2 W m^{-2} LWIR flux from all of the increase in atmospheric CO_2 concentration over the last 200 years.

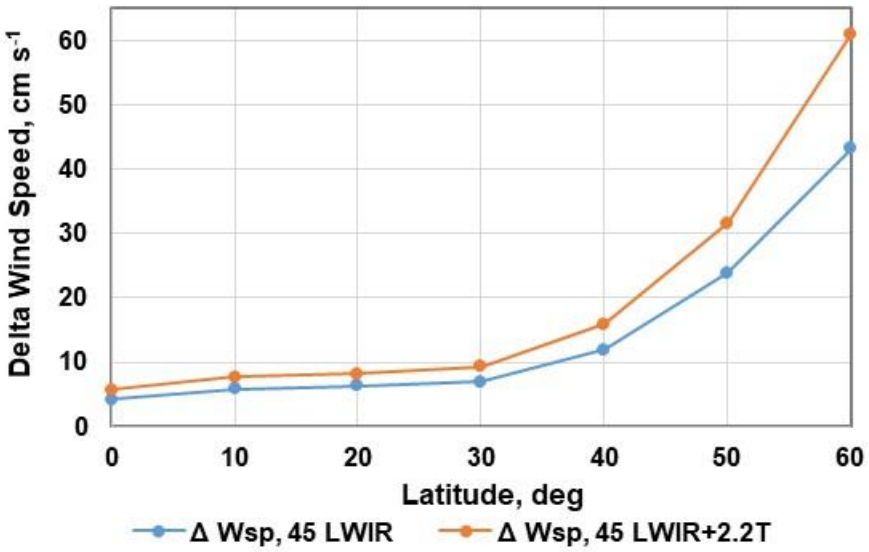

Figure 1: Change in wind speed (cm s^{-1}) needed to restore the ocean surface cooling flux when the downward LWIR flux is increased by 2 W m^{-2}. Both the fixed and the temperature dependent LWIR window flux cases are shown.

The effect of the variable wind speed on the ocean evaporation may be evaluated by adding random number generators to the model wind speed and LWIR flux. The wind speed was randomly varied daily by up to ±4 m s^{-1}, and in each half hour step by up to 1 m s^{-1}. The LWIR flux was varied in each half hour step by up to ±10 W m^{-2}. The model was run for 30 years for 3 cases, 1) LWIR window set to 45 W m^{-2}; 2) LWIR window set to 43 W m^{-2} and 3) 43 W m^{-2}, with wind coupling constant adjusted to return the temperatures back to the 45 W m^{-2} case. The latitude was set to 20° and the daily minimum and maximum surface temperatures were extracted from the output data. The 30 year averages and standard deviations were calculated for each day. The averages and the ±1 σ ranges for the minimum and maximum surface temperatures for the 3 cases are plotted in Figure 2. The plots overlap well within the 1σ standard deviation limits.

The small surface temperature changes produced by this dynamic thermal reservoir model when the LWIR flux is changed by 2 W m^{-2} clearly demonstrate that the equilibrium atmosphere assumption is invalid. There can be no 'climate sensitivity' to a doubling of the atmospheric CO_2 concentration. Nor can there be any 'water vapor feedback'. In practice, the normal day to day variations in the surface flux terms are so large that any small increase in the LWIR flux from CO_2 cannot produce an observable increase in the measured ocean surface temperature or MSAT.

Further analysis of ocean and land temperatures, including the convection transition temperature and the phase shift is provided by Clark [2019a, b]

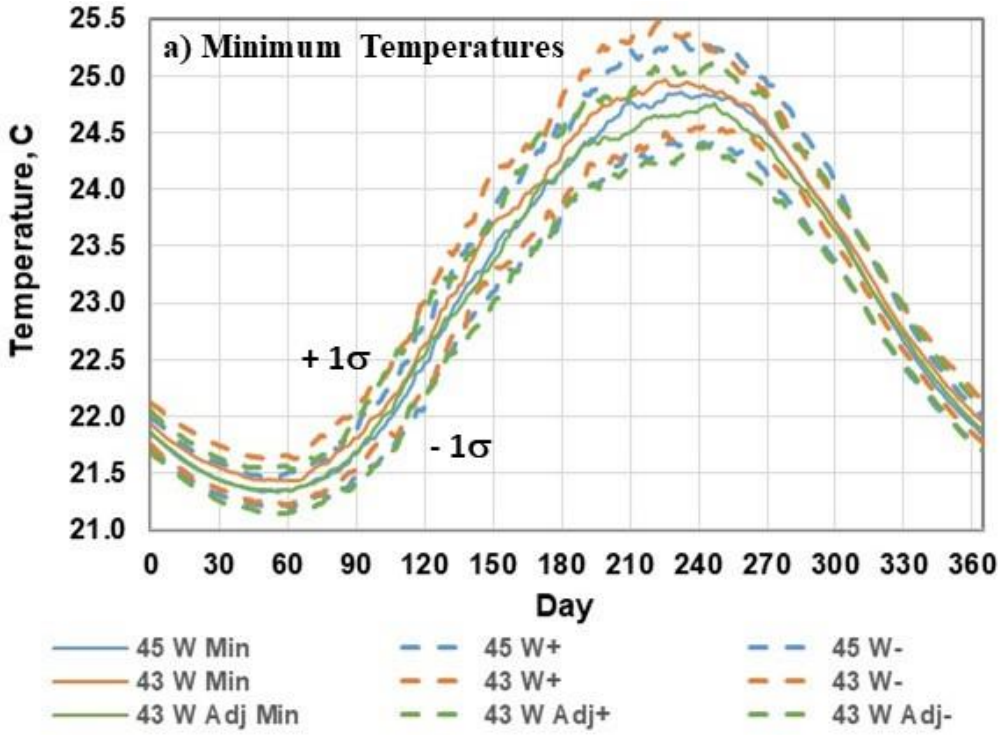

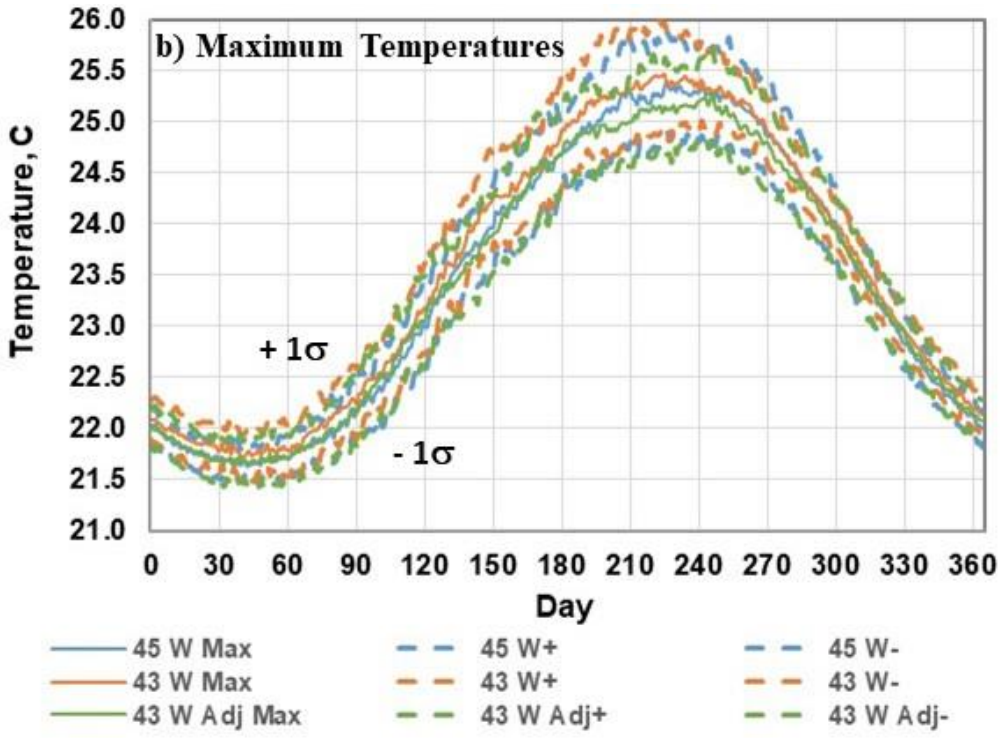

Figure 2: 30 year averages and 1 σ standard deviations for cases 1 through 3, 20° latitude, minimum and maximum temperatures with random number generators to simulate changes in wind speed and LWIR flux.

Part 2: The observed recovery in surface temperature since the Maunder minimum can be explained in terms of small increases in the solar flux absorbed and accumulated in the ocean thermal reservoir.

The analysis of surface temperature using thermal engineering models based on dynamically coupled thermal reservoirs, has demonstrated the first part of the null hypothesis. The increase of approximately 2 W m^{-2} in the downward LWIR flux to the surface produced by observed increase of 120 ppm in the atmospheric CO_2 concentration cannot couple into climate system in a way that can cause any observable climate change. The coupling of the solar flux into the oceans is now considered. In particular, how do small changes in the solar flux cause climate change?

The starting point is to estimate the solar flux levels need to bring the earth out of an Ice Age and to warm the earth from the Maunder minimum. These simple calculations clearly show that the observed temperature changes are caused by small solar flux changes accumulated over time. Next, the solar flux algorithm in the land and ocean surface temperature models is used to calculate the change in surface flux produced by a change of 1 W m^{-2} in the average incoming TOA flux. The changes in solar flux are produced by two different mechanisms. The variation in the earth's orbital ellipticity, obliquity and precession (Milankovitch cycles) produce changes in the TOA flux intensity that do not alter the spectral distribution. However, the TOA flux changes produced by

variations in the sunspot index and related parameters do change the spectral properties of the solar flux. Almost of the observed changes occur in the blue and UV parts of the solar spectrum.

The coupling of the solar flux into the oceans is complex. The trade winds produced by the Hadley, Ferrell and Polar convective cell structure drive five major ocean gyres. In the eastern parts of the equatorial Atlantic and Pacific Oceans, the wind driven surface evaporation is insufficient to remove the tropical solar heat and the ocean water transported westwards by the equatorial currents must heat up. This leads to the formation of the tropical warm pools in the western Atlantic and Pacific Oceans [Clark, 2019b]. The warm water is then transported poleward by the western boundary currents and recirculated through the gyres. These western currents run fast and deep so that some of the warmer water is forced below the normal gyre circulation. There is never an exact balance between the solar heating and the wind driven cooling. This means that the ocean surface temperatures must oscillate. These are quasi-periodic oscillations that do not have a fixed frequency. The El Nino Southern Oscillation (ENSO) in the equatorial Pacific Ocean has a period between 3 and 7 years. The Pacific Decadal oscillation (PDO) and the Atlantic Multi-decadal Oscillation (AMO) have periods in the 60 to 70 year range.

During the last glacial maximum, sea level was 120 m lower than it is now [Lambeck, 2004]. This water was stored at higher latitudes as freshwater ice. The amount of heat needed to melt a column of ice 120 m high with a 1 m^2 cross section and heat the melt water from 0 to 15 C is approximately 3.7 x 10^4 MJ. To melt this ice over a period of 10,000 years, a 24 hour average flux of 0.12 W m^{-2} is needed, coupled directly into the ice sheet.

Since 1850, ocean surface temperatures have warmed by approximately 0.7 C based on a simple linear fit to the HadSST3 ocean temperature anomaly [HadSST3, 2019]. Assuming a uniform temperature increase in the first 100 m depth, this requires the addition of 293 MJ of heat per square meter x 100 m column. Since 1850, this requires a 24 hour average flux of approximately 0.06 W m^{-2} coupled to the surface.

Using the 'clean air' solar flux algorithm from IEEE Standard 378 [IEEE 1993], the change in the surface flux produced by an increase of 1 W m^{-2} in TOA flux may be estimated. The calculated average daily cumulative flux vs. latitude is divided by 1365 to get to the 1 W m^{-2} TOA flux level. This is then scaled by a factor of 0.7 to account for cloud attenuation. These flux values can then be compared to the 0.12 W m^{-2} needed to bring the earth out of an Ice Age. The flux has to be reduced by another factor of 0.7 to account for the additional short wavelength atmospheric attenuation [ASTM, 2012]. These values can then be compared to the 0.06 W m^{-2} need for the earth to recover from the Maunder minimum. This is shown in Figure 3. While these are very approximate estimates, the small changes in flux accumulated over long periods of time are consistent with the observed warming and provide the justification for further investigation. In particular, more detailed estimates of the ocean heating, sunspot induced flux changes and other possible heating and feedback mechanisms are needed. Most of the ocean heating reported by Levitus et al has occurred since 1985 and is probably caused by warm phase ENSO and related ocean oscillations [NOAA, Ocean heat content, 2019; Levitus et al, 2012]. The warm surface

water is coupled to lower depths by Ekman transport and Ekman pumping [NOAA 2019, Ekman Transport].

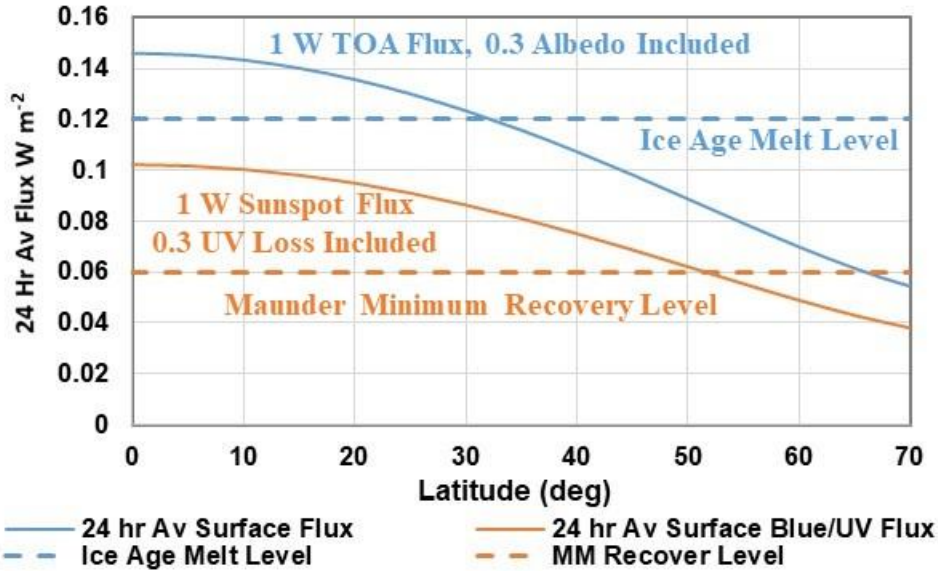

Figure 3: 24 hr average surface flux change produced by a 1 W m^{-2} change in solar flux estimated from the IEEE 738 solar algorithm. Blue line with 0.7 albedo added. Orange line with an additional 0.7 atmospheric transmission reduction included. Dotted lines are estimated Ice Age melt and Maunder minimum warming flux levels.

Using VIRGO radiometer data from the SOHO satellite, a change in the sunspot index of 100 produces a change in solar flux of approximately 1 W m^{-2} in the top of atmosphere (TOA) solar flux [VIRGO, 2017]. It should be noted that the sunspot index was revised in 2015 to Version 2 [SILSO, 2019; Lockwood et al, 2016]. This revision increased the sunspot number values by approximately 1.6. The analysis here is based on the version 1 index. The VIRGO data and the corresponding sunspot index are shown in Figure 4. In addition to the change from the sunspot index, there was an overall increase in brightness in the TOA flux during the recovery from the maunder minimum. This is shown in Figure 5. The upper trace, Figure 5a shows the TOA response at all wavelengths. The lower 3 traces, Figures 5b though 5d show the TOA response in spectral bands at 0.12 to 0.4 μm, 0.4 to 1 μm and 1 to 100 μm. The largest changes are at the shorter wavelengths.

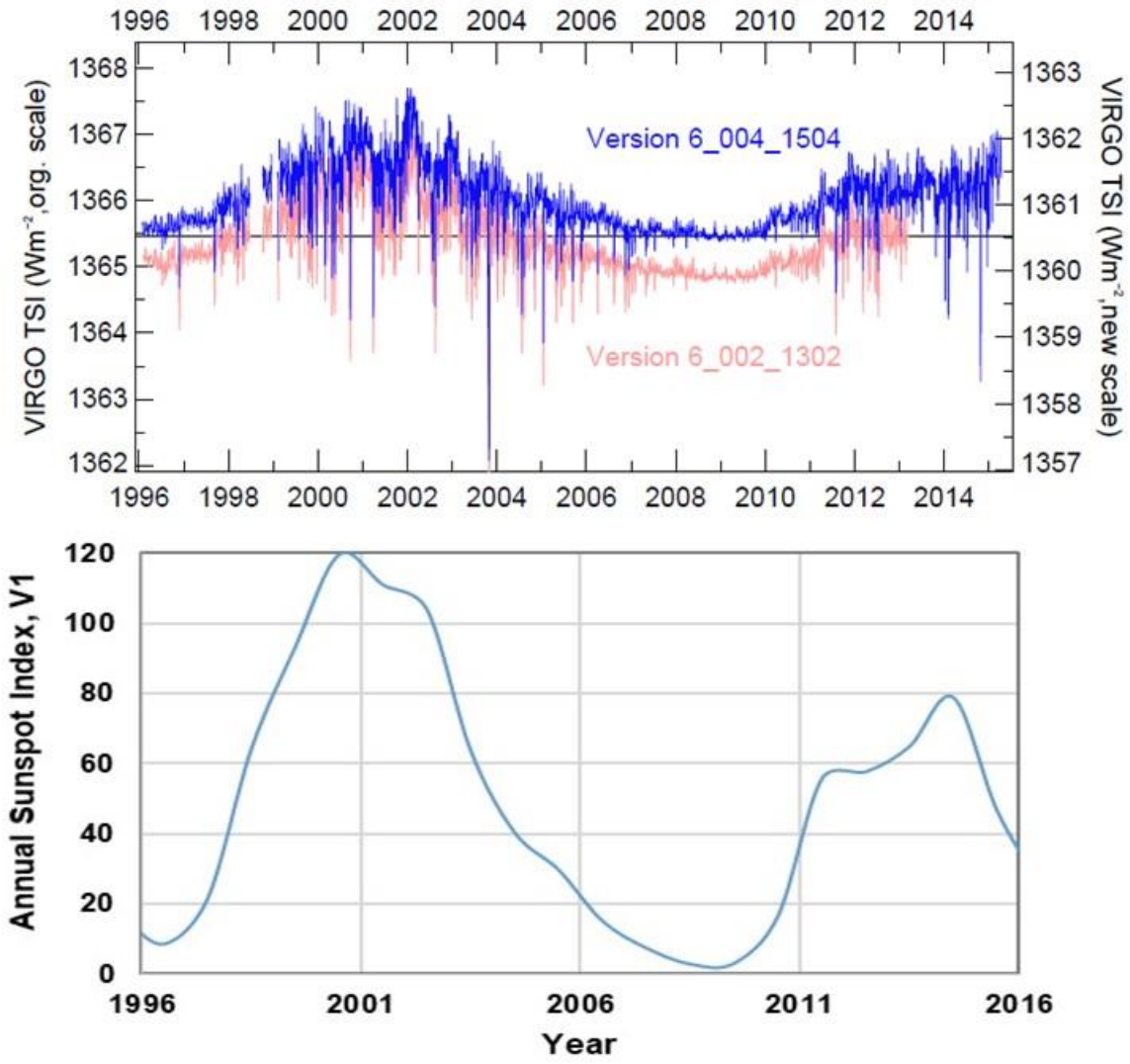

Figure 4: VIRGO radiometer data and the sunspot index used to estimate the sunspot induced change in the solar flux. A change in index of 100 is assumed to produce a change of 1 W m^{-2} in the TOA flux.

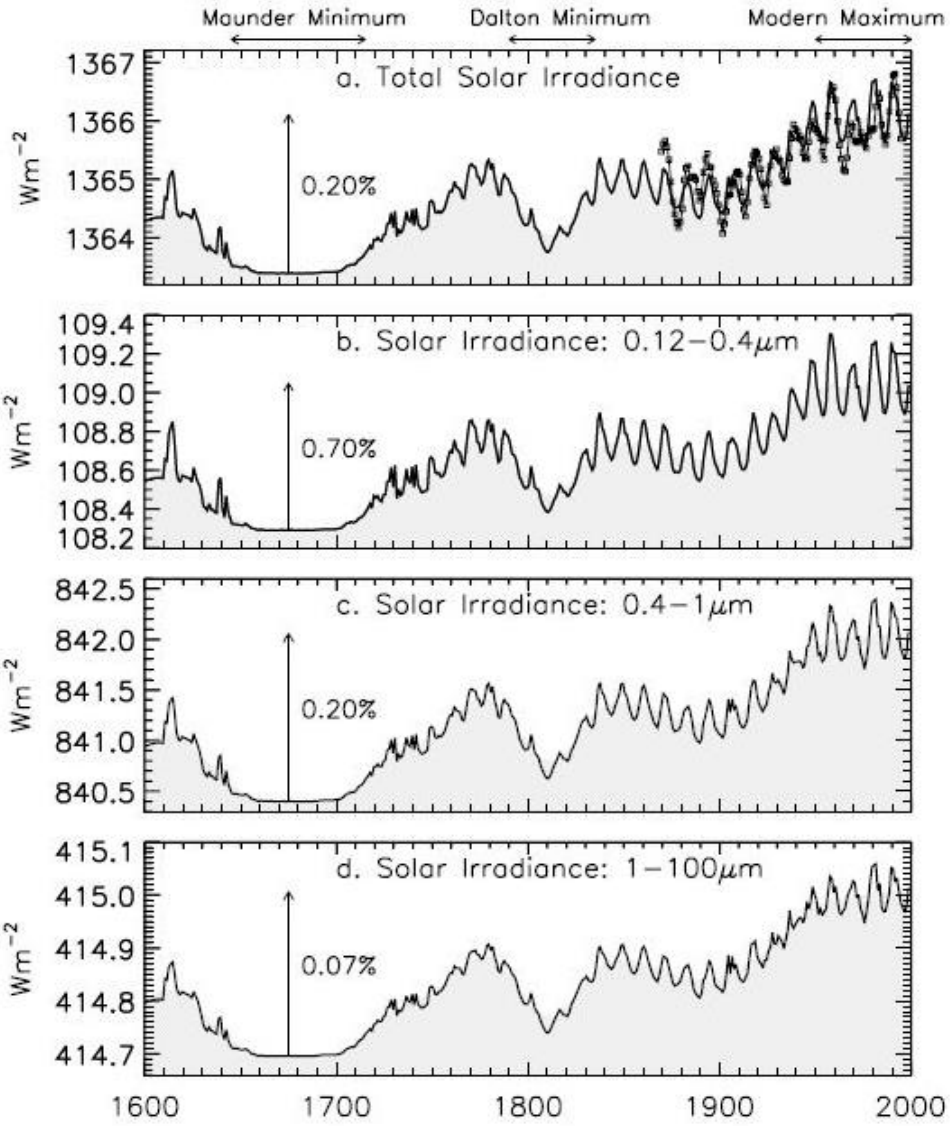

Figure 5: Estimated changes in the total solar irradiance and in selected spectral regions since the Maunder minimum [Lean, 2000].

Based on Figures 4 and 5, the increase in solar flux from 1850 may be estimated by dividing the sunspot index by 100 and adding an offset of 0.5. The annual values were added year by year to obtain the cumulative increase. This was then scaled using a least squares fitting approach to match the HadSTT3 global ocean surface temperature anomaly series [HadSST3, 2019]. The best fit was y = 0.00384 cum – 0.421. For comparison, the Excel Trendline™ linear fit to the HadSST3 data gave a slope of 0.0042 or an ocean surface temperature increase of 0.42 C per century. This is shown in Figure 6. From Figure 3 above, the approximate increase in a 24 hour average solar sunspot flux (orange line) produced by a 1 W increase in TOA flux is 0.08 W m^{-2}. When this is coupled into a 100 m column of water over 150 years, the estimated temperature rise is 1.06 C. While these are rather approximate numbers, they are consistent with the increase in solar sunspot

flux as the ocean heating mechanism responsible for the temperature recovery from the Maunder minimum. This is discussed in more detail by Clark [2019b]

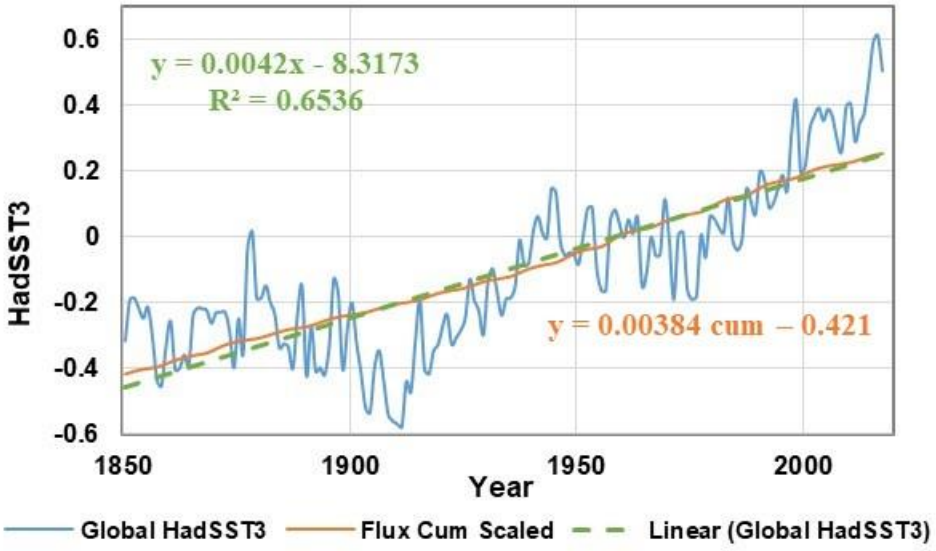

Figure 6: HadSST3 global ocean surface temperature index since 1850, linear fit to HadSST3 and best least squared fit to the scaled cumulative sunspot flux.

Changes in cloud cover related to cosmic ray seeding have been proposed as a mechanism for climate change [Svensmark, 2017; 2009]. Cosmic ray seeding increases as sunspot activity decreases. However, this does not account for the full cloud cycle. Clouds are formed, they can be transported over long distances by weather systems and they dissipate through deposition and evaporation. Seeding by cosmic rays increases the initial cloud cover in regions at saturation, but the effects on cloud lifetime and transport have not been considered. The extra cloud formation also has to block additional sunlight, so this does not impact regions that already have 100 % cloud cover. These increases in cloud cover can also increase the downward LWIR flux to the surface and reduce surface cooling. Any changes in ocean heating may also influence the wind speed. Further analysis of cosmic ray seeding is needed that includes the full cloud cycle and the detailed surface energy transfer.

Cosmic ray seeding is associated with climate changes such as the Maunder minimum and the medieval and modern warming periods. Longer term climate changes such the 100,000 year Ice Age cycle are produced by planetary perturbations to the earth's orbital and axial motion. These do not involve changes in solar activity and should not be influenced by cosmic ray seeding.

Longer Term Climate Changes

Changes in the solar flux related to the sunspot cycle have produced climate change over time scales of a few hundred years including the medieval maximum, the Maunder minimum and the modern solar maximum. Planetary perturbations of the earth's orbit, mainly by Jupiter have

produced climate change related to variations in the Earth's orbital ellipticity, and axial tilt and precession. These are known as Milankovitch cycles [2019]. Currently, the change in ellipticity is dominant and cycles the earth through an Ice Age in about 100,000 years. Over longer time periods, climate change is also caused by variations in ocean circulation as the continental boundaries change with plate tectonic motion. Major climate shifts were caused by the opening the Drake Passage to form the Southern Ocean and by the formation of the Isthmus of Panama.

In much earlier geological times, 2.5 billion years ago, the solar flux was about 80% of its current level. This leads to the called 'faint sun paradox'. Using conventional equilibrium greenhouse effect arguments, the earth should have been much cooler than it was [Goldblatt & Zahnle, 2011]. This may be resolved using the coupled thermal reservoir approach. Ocean temperatures are set by wind driven evaporation, not by IR thermal equilibrium.

These longer term climate changes have been discussed in more detail by Clark [2019b, d]

References

ASTM, 2012, G173-3, Solar reference spectra AM1.5, http://rredc.nrel.gov/solar/spectra/am1.5/

Christy, J. R., GWPF Note 17, 2019, 'The Tropical Skies, Falsifying Climate Alarm', https://www.thegwpf.org/content/uploads/2019/05/JohnChristy-Parliament.pdf

Clark, R. 2019a, '*A Dynamic Coupled Thermal Reservoir Approach to Atmospheric Energy Transfer Part III: The surface Temperature*', Ventura Photonics Monograph, VPM 004.1, Thousand Oaks, CA, May 2019

http://venturaphotonics.com/files/CoupledThermalReservoir_Part_III_Surface_Temperature.pdf

Clark, R. 2019b, '*A Dynamic Coupled Thermal Reservoir Approach to Atmospheric Energy Transfer Part IV: The Null Hypothesis for CO_2*' Ventura Photonics Monograph, VPM 005.1, Thousand Oaks, CA, May 2019

http://venturaphotonics.com/files/CoupledThermalReservoir_Part_IV_The_Null_Hypothesis.pdf

Clark, R. 2019c, '*A Dynamic Coupled Thermal Reservoir Approach to Atmospheric Energy Transfer Part V: Summary*', Ventura Photonics Monograph, VPM 006, Thousand Oaks, CA, May 2019

http://venturaphotonics.com/files/CoupledThermalReservoir_Part_V_Summary.pdf

Clark, R. 2019d, '*The Greenhouse Effect*', Ventura Photonics Monograph, VPM 003.2, Thousand Oaks, CA, May 2019

http://venturaphotonics.com/files/The_Greenhouse_Effect.pdf

Clark, R. 2019e, '*50 Years of Climate Fraud*', Ventura Photonics Monograph, VPM 002.1, Thousand Oaks, CA, May 2019

http://venturaphotonics.com/files/50_Years_of_Climate_Fraud.pdf

Clark, R., 2013a, Energy and Environment **24**(3, 4) 319-340 (2013), 'A dynamic coupled thermal reservoir approach to atmospheric energy transfer Part I: Concepts'

http://venturaphotonics.com/files/CoupledThermalReservoir_Part_I_E_EDraft.pdf

Clark, R., 2013b, Energy and Environment **24**(3, 4) 341-359 (2013) 'A dynamic coupled thermal reservoir approach to atmospheric energy transfer Part II: Applications'

http://venturaphotonics.com/files/CoupledThermalReservoir_Part_II__E_EDraft.pdf

Goldblatt, C. and K. J. Zahnle, Clim. Past **7** 203-220 (2011), 'Clouds and the faint young sun paradox'.

HadSST3, 2019, https://crudata.uea.ac.uk/cru/data/temperature/HadSST3-gl.dat

Hale, G. M. and Querry, M. R., Applied Optics, **12**(3) 555-563 (1973), 'Optical constants of water in the 200 nm to 200 μm region'

Harde, H., Int. J. Atmos. Sci.9251034 (2017), 'Radiation Transfer Calculations and Assessment of Global Warming by CO_2' https://doi.org/10.1155/2017/9251034

IEEE, IEEE Std 738-1993, *IEEE Standard for calculating the current temperature relationship of bare overhead conductors*

IPCC, 2013: *Climate Change 2013: The Physical Science Basis. Contribution of Working Group I to the Fifth Assessment Report of the Intergovernmental Panel on Climate Change* [Stocker, T.F., D. Qin, G-K. Plattner, M. Tignor, S.K. Allen, J. Boschung, A. Nauels, Y. Xia, V. Bex and P.M. Midgley (eds.)]. Cambridge University Press, Cambridge, United Kingdom and New York, NY, USA, 1535 pp, doi:10.1017/CBO9781107415324.

http://www.climatechange2013.org/report/full-report/

Keeling, 2019, https://scripps.ucsd.edu/programs/keelingcurve/

Lambeck, K., Comptes Rendus Geoscience **336** 667-689 (2004), 'Sea level change through the last glacial cycle: geophysical, glaciological and paleo-geographic consequences'

Lean, J. Geophys Res. Letts. **27**(16) 2425-2428 (2000), 'Evolution of the sun's spectral irradiance since the Maunder minimum'

https://agupubs.onlinelibrary.wiley.com/doi/epdf/10.1029/2000GL000043

Levitus, S. et al, (11 Authors), Geophysical Research Letters, **39** L10603 1-5 (plus auxiliary material) (2012) 'World ocean heat content and thermosteric sea level change (0-2000 m), 1955-2010'

Lockwood, M.; M. J. Owens, L. Barnard and I. G. Usoskin, The Astrophysical Journal **824**:54, 17pp, June10 (2016) doi:10.3847/0004-637X/824/1/54, 'An assessment of sunspot number data composites over 1845-2014,'

http://iopscience.iop.org/article/10.3847/0004-637X/824/1/54/pdf

Milankovitch Cycles, 2019, https://en.wikipedia.org/wiki/Milankovitch_cycles

NOAA, 2019, Ocean Heat Content, https://www.ncdc.noaa.gov/cdr/oceanic/ocean-heat-content

NOAA, 2019, Ekman Transport, http://oceanmotion.org/html/background/ocean-in-motion.htm

SILSO, 2019, http://www.sidc.be/silso/datafiles

Spencer, R. W., 2013, STILL Epic Fail: 73 Climate Models vs. Measurements, Running 5-Year Means June, 2013. http://www.drroyspencer.com/2013/06/still-epic-fail-73-climate-models-vs-measurements-running-5-year-means/

Svensmark, H.; T. Bondo & J. Svensmark, Geophys. Res. Letts. **36** L15101 pp1-4 (2009), 'Cosmic ray decreases affect atmospheric aerosols and clouds'

Svensmark, H.; M. B. Enghoff, N. J. Shaviv & J. Svensmark, Nature Communications **8**:2199 doi:10.1038/s41467-017-02082-2 (2017), Increased ionization supports growth of aerosols into cloud condensation nuclei' https://www.nature.com/articles/s41467-017-02082-2

VIRGO, 2017, SOHO Satellite VIRO Radiometer Data,

http://www.pmodwrc.ch/pmod.php?topic=tsi/virgo/proj_space_virgo#VIRGO_Radiometry

Zachos, J.; M. Pagani, L. Sloan, E. Thomas and K. Billups, Science **292** 686-689 (2001), 'Trends, rhythms and aberrations in the global climate, 65 Ma to present'